ISBN: 978-3-95450-184-7 doi:10.18429/JACoW-IPAC2018-THPAL025

NEW DRIFT-TUBE LINAC RF SYSTEMS AT LANSCE*

J. Lyles†, R. Bratton, M. Prokop, D. Rees
Los Alamos National Laboratory, Los Alamos, NM 87545 USA

Abstract

LANSCE has restored the proton drift-tube linac (DTL) to high-power capability after the original RF-power tube manufacturer could no longer supply devices that consistently met our high-average power requirement. Thales TH628L Diacrodes® now supply RF power to three of the four DTL tanks. These tetrodes reused the existing infrastructure including water-cooling systems, coaxial transmission lines, high-voltage power supplies and capacitor banks. Each transmitter uses a combined pair of power amplifiers to produce up to 3 MW peak and 360 kW of mean power. A new intermediate power amplifier (IPA) was simultaneously developed using a TH781 tetrode. Design and prototype testing of the high-power stages was completed in 2012, with commercialization following in 2013. Each installation was accomplished during a 4 to 5 month beam outage each year from 2014-2016. A new digital low-level RF control system was designed, built and placed into operation in 2016. The interaction of the dual power amplifiers, the I/Q LLRF, and the DTL cavities provided many challenges that were overcome. The replacement RF systems have completely met our accelerator requirements. Lessons learned from our experience are shared here.

COMPONENTS AND INTERACTIONS

The LANSCE DTL uses four Alvarez cavities powered at 201.25 MHz, to accelerate both protons (H^+) and hydrogen ions (H^-) from 0.75 to 100 MeV before injection into a coupled-cavity linac (CCL). Pulsed RF systems are capable of 12% duty factor and nominally 3 MW of peak RF power, with corresponding average power capability of 360 kW per cavity. Previous reports [1, 2, 3] discussed the benefits of using the TH628L Diacrode® from Thales Electron Tubes as the active device for this application. Combining the outputs of two PAs provided ample headroom in peak and average power, allowing the tubes to operate safely within their rating [4]. Amplifier reliability and tube lifetime are both improved from these new systems. In April of 2018, there were 6 Diacrodes® operating with a range of 11,363-23,824 hours without needing filament power adjustment. The integration of a new digital low-level RF (dLLRF) controller for each transmitter was completed in 2016. Experience from this work identified improvements that were made to the RF transmission infrastructure, amplifier protection logic, and dLLRF algorithms and timing.

Coaxial Transmission Lines

The IPA for each transmitter nominally operates from 80-120 kW as needed for the final stage power of 2-3 MW driving each DTL cavity. Figure 1 is a block diagram of the cascade of amplifiers. The IPA feeds power to a λ/4 coupled-line hybrid to develop power for both final power amplifiers (FPA). One path has a passive high-power phase shifter with +/- 10 degrees of mechanical adjustment and the other has a fixed length to compensate for the shifter's midpoint delay. The outputs from the two FPA are combined in a λ/4 branch-line hybrid made from 30.5 cm (12 in) diameter coaxial line. Matched directional couplers feed phase-stable coax to a custom-pulsed phase meter. This novel vector voltmeter uses the AD8302 phase detector integrated circuit along with a FPGA and a digital display of +/- 10 degrees. This diagnostic allows for real time adjustment of intra-amplifier phasing using the passive phase adjuster. At 200 MHz, 1 cm of coax length is equivalent to 2.4 degrees of phase. These devices allow optimizing the power combining to account for mechanical tolerances of the transmission lines at each transmitter.

There are no circulators used in the new RF plant. The hybrids are reciprocal devices, so the power combiner also splits reflected power from the DTL into quadrature components at the two Diacrodes®. This causes difficulty in maintaining equal power balanced between amplifiers as each tube operates into a different phase of mismatch. To resolve this problem, a separate λ/4 electrical delay is placed in the 23.3 cm (9 in) diameter coaxial line from one FPA to force the two tubes to drive identical complex impedances. This re-phasing would upset the combiner unless a similar delay is placed in the input line of the opposite amplifier. It re-establishes the quadrature relationship at the two inputs at the branch-line combiner. Mega Industries provided the custom components and largest diameter coaxial lines. Myat and Connecticut Microwave provided the balance of the items that had EIA standard flanges. The original 35.5 cm (14 in) diameter transmission line is connected to the output of the branch-line combiner to drive the DTL power coupler.

Re-phasing between the amplifiers is not sufficient to ensure satisfactory system operation with reflected power. It is well known that a tube amplifier should be positioned at multiples of λ/2 from the power coupler. This ensures that the RF voltage inside the active region of the tube does not rise when there is a spark inside the DTL, from impedance inversion. The correct choice of line length reduces tube gain during reflected power events from

* Work supported by the United States Department of Energy, National Nuclear Security Agency, under contract DE-AC52-06NA25396
# jtml@lanl.gov

ISBN: 978-3-95450-184-7 doi:10.18429/JACoW-IPAC2018-THPAL025

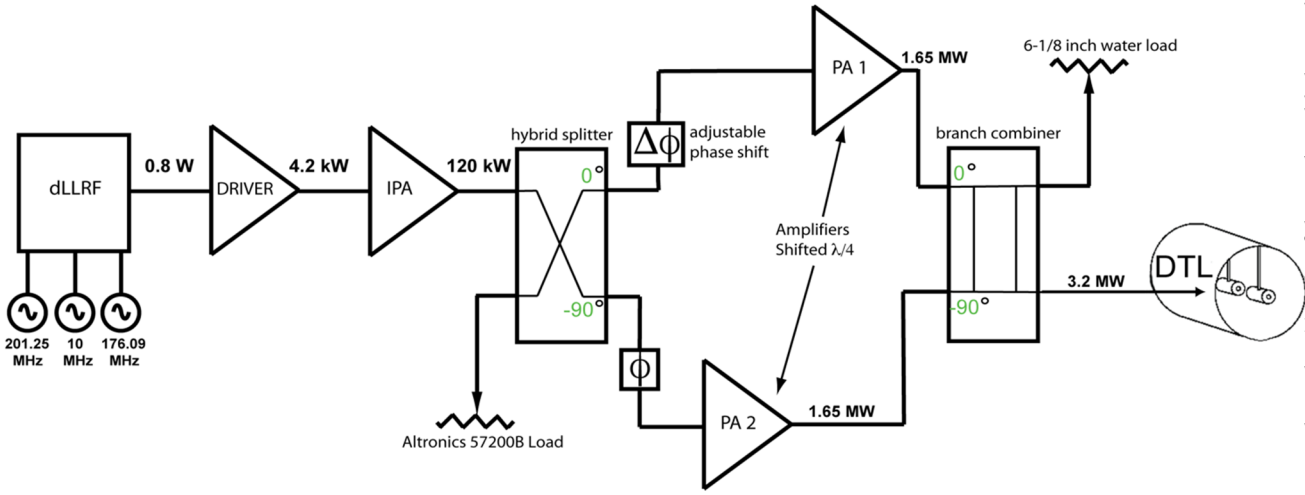

Figure 1: Diagram of 201 MHz RF system with power-combined final amplifiers.

the DTL. A solution was added to the 23.3 cm (9 in) coaxial output feeders, with identical lengths applied to the output of each FPA. This modification requires that the dLLRF must generate the initial ramp-up of RF power without tight feedback gain control, to prevent overdriving the amplifiers during the transient reflected power peak on the front end of every pulse.

Fast Protect and Monitoring System

FPMS was designed to provide fast protection of the amplifiers and Linac from critical tube current and RF power faults. This FPGA-based logic system is reprogrammable to accommodate changes in functionality. It displays RF peak power levels for eight directional couplers per FPA, indexed by an adjustable sample gate during the RF pulse. FPMS provides timing for the grid bias voltage pulses in the tubes and the RF drive from dLLRF. In the event of faults, it can quench these signals in less than 3 μS. The RF power sensors were developed using the ADL5510 envelope detector integrated circuit along with an embedded PIC microprocessor. This has sufficient accuracy and wide dynamic range to rival commercial power meters and is much less expensive. The PIC handles calibration terms and offset values and then sends the peak value via serial interface for display on the front panel of FPMS. As we first operated these systems, we determined the best settings for RF protection. Reflected power trip levels were chosen to be 200 kW peak. To allow the turn-on and turn-off reflected power excursions to exceed this value, a blanking signal is provided so that the sensors are ignored during the ramp times. All of this timing is adjustable through an EPICS GUI.

RF fault conditions immediately turn off the RF drive and lower the grid bias for all tubes to cut-off voltage, then recover them on the next pulse, ~8 mS later. Certain signals, such as DTL and FPA reflected powers, can retry 6 times on sequential pulses before shutting off the RF command switch to require operator intervention. Other signals such as tube over-currents will turn the system off immediately on the first occurrence. In addition, a fast crowbar can fire to discharge the anode capacitor bank. A new signal was added in 2017 from a detector generating the derivative of the DTL field sample. This voltage is compared to a threshold and the resultant provides another logic turnoff signal. So far it has only been used to trigger oscilloscopes and counters to record DTL sparks in one particularly troublesome tank. We expect to integrate this protection into the fast shutdown logic in 2018 with a firmware update.

Digital Low Level RF Controller

The original analog amplitude and phase control electronics were replaced with dLLRF, using down/up conversion to ~25 MHz, where the demod/modulation functions are implemented using the I/Q sampled method [5]. The basic controls and signal processing are accomplished using FPGAs [6]. Embedded EPICS allows setting of control parameters and uploading of waveforms. PI algorithms work on the I and Q data with feedback from a DTL sample. Two feedforward terms are also used, one being a beam current signal from a pickup at the LEBT and another using iterative learning from previous pulses. The dLLRF supplies vector modulated RF drive to the first linear transistor preamp/driver stage, a 5.5 kW amplifier from Communications Power Corporation.

Timing in the PI controller is set so that a steering signal first drives the RF ramp up. At the beginning of flattop, the PI gains are enabled to stabilize the field. Figure 2 shows the resultant waveforms captured at the third DTL cavity, where the green trace is a sample of the field, the blue is total forward power from the combined amplifiers, and red is total reflected power. These are detected RF power signals from the ADL5511 envelope detectors. Beam loading is apparent, where the forward power increases. A troublesome spike in the reflected power at the middle of ramp-down was due to the Diacrode® control grid voltage switching to cut-off level early. Ramp length and type of ramp influenced the magnitude and timing of the initial reflected power transient. A special ramp with a

ISBN: 978-3-95450-184-7 doi:10.18429/JACoW-IPAC2018-THPAL025

gradual rollover to flattop was developed to improve this.

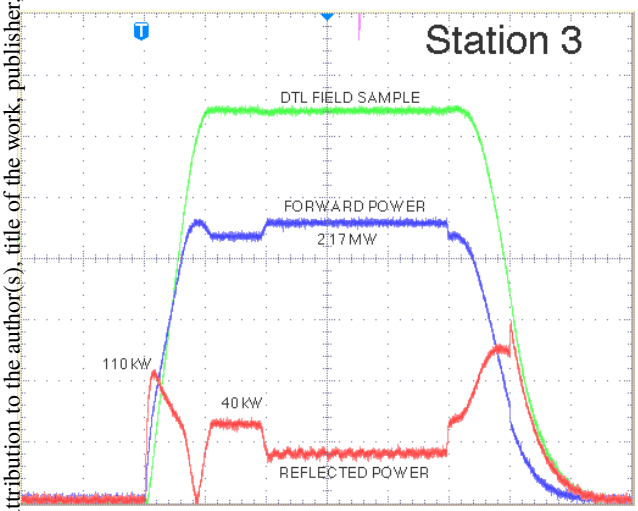

Figure 2: Normal operation with beam in 2017.

For turnoff, it was always felt that the approach with the least reflected power was optimal. This was produced with the inverse of the turn on ramp. The waveforms in Fig. 3 are similar to Fig. 2 without beam, and field sample is offset (top trace). The peak in reflected power (bottom trace) represents 145 kW. Forward power (middle trace) at this same time is 530 kW. This creates a large standing wave in the power coupler, transmission lines, power combiner, and power amplifier, and the voltage standing wave ratio (VSWR) is 3.2:1. During flattop, forward power is 1.95 MW and reflected is 40 kW, for VSWR of 1.32:1. Beam loading improves this.

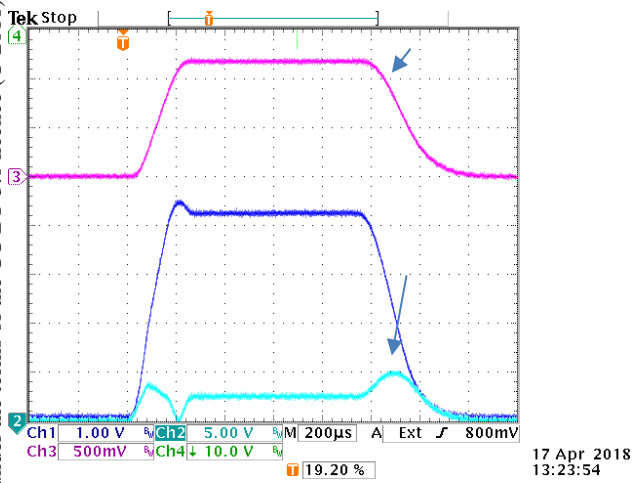

Figure 3: Detected envelopes of RF power with similar ramps on both ends of the pulse, arrows at high VSWR.

DTL 3 was having frequent internal sparks around this point in the ramp down. A test was developed using fast shut off of the RF with a PIN diode switch in the dLLRF output. This resulted in the waveforms of Fig. 4. The reflected power scale was increased by 2.5 times compared to Fig. 3. Immediately before the sharp peak in reflected power, the measured forward power is 620 kW. Reflected power a few microseconds later is 610 kW and forward is very low. This infers that there is insignificant standing wave and the reflected power is a travelling wave directed towards the amplifier from the stored energy in the cavity. Operating in this manner has resulted in significant reduction in spark overs. There are very few at turnoff, as a result of the improvement. We will continue to operate one system like this, before converting the other two.

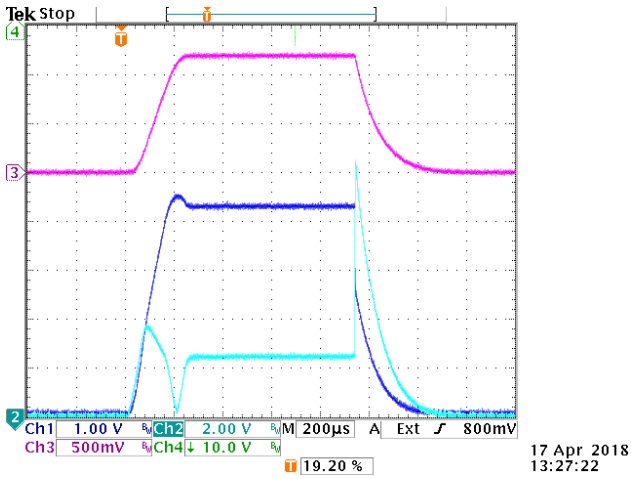

Figure 4: Detected envelopes of RF power with ramp at start and fast shut-off at end of pulse.

Helpful Diagnostics for this Process

Several new diagnostics were developed over this same period of time, 2014-2018. Precise independent phase detectors using AD8302 are installed that compare the pulsed RF field sample to the master oscillator. These can resolve 0.1 degrees difference across a pulse. They helped immensely in improving the dLLRF phase control response. Similarly, precise amplitude detectors have been developed using ADL5511 envelope detectors to verify amplitude stability. For the troublesome DTL cavity 3, infrared pickups have been added to view inside at 6 locations through small quartz windows, installed in extra RF sampling loop ports. The light is detected remotely by Advanced Ferrite Technology arc detector electronics and the analog voltage is displayed on an 8-channel oscilloscope. From these we determine approximately where any sparking is happening. X-ray detectors have also been used to record the longitudinal field uniformity.

CONCLUSION

The interaction of new dual power amplifiers through the transmission lines and power combiner, dLLRF, and room temperature Alvarez DTL cavities have provided significant challenges that were overcome at LANSCE. Many adjustments were required from LLRF though high power, before declaring success with these new 201 MHz RF systems. It is hoped that this report can assist others attempting similar complex installations, merging new high power RF amplifiers and control systems with older linacs.

ISBN: 978-3-95450-184-7 doi:10.18429/JACoW-IPAC2018-THPAL025

REFERENCES

[1] G. Clerc, J. P Ichac, C. Robert, “A New Generation of Gridded Tubes for Higher Power and Higher Frequencies”, in *Proc. PAC’97*, Vancouver, BC, Canada, May 1997, pp. 2899-2901.

[2] M. Grezaud, A. Boussaton, C. Robert, "TH628L Diacrode Status", *International Vacuum Electronics Conference*, Monterey, CA, USA, Apr. 2014, pp. 111-112.

[3] J. Lyles, W. Barkley, J. Davis *et al.*, “System Considerations for 201.25 MHz RF System for LANSCE”, in *Proc. NA/PAC’13*, Pasadena, CA, USA, Oct. 2013, pp. 963-965.

[4] J. Lyles, Z. Chen, J. Davis *et al.*, “Design, Test and Implementation of New 201.25 MHz RF Power Amplifier for the LANSCE Linac”, in *Proc. IPAC’12*, New Orleans, LA, USA, May, 2012, pp. 3446-3448.

[5] J. Lyles, W. Barkley, R. Bratton, M. Prokop, D. Rees, “Design, Fabrication, Installation and Operation of New 201 MHz RF System at LANSCE”, in *Proc. LINAC ’16*, East Lansing, MI, USA, Sep. 2016, pp. 3446-3448.

[6] S. Kwon, L. Castellano, D. Knapp *et al.*, “FPGA Implementation of a Control System for the LANSCE Accelerator”, in *Proc. IPAC’16*, Busan, Korea, May, 2016, pp. 2771-2773.